Proceedings of Ninth World Conference on Earthquake Engineering
August 2-9, 1988, Tokyo-Kyoto, JAPAN (Vol.II)

3-4-1

STATISTICAL CHARACTERISTICS OF SEISMIC WAVE PROPAGATION IN SOIL WITH VERTICAL INSTRUMENTS ARRAY

Satoshi KURITA[1], Masanori IZUMI[1], Setuo IIZUKA[2],
Toshimi SATO[3] and Tomoki AIBA[1]

1 Faculty of Engineering, Tohoku university, Sendai, Japan
2 Tohoku Electric Power Co. Ltd., Sendai, Japan
3 Shimizu Cooperation, Tokyo, Japan

SUMMARY

Through applying statistical analyses,we investigate the multi-dimensional seismic wave propagation by examining the observed motions. The results of the cross correlation analyses suggest that there are shear waves having high correlation between the different orthogonal components at vertical points. By estimating the transfer functions and coherence functions for the various spectra of the motion vectors, it is shown that shear waves propagate through subsurface layers with changing the direction of motions. It is concluded that this multi-dimensional wave propagation phenomenon can be explained in terms of irregularities of the soil structure.

INTRODUCTION

In order to develop accurate methods to generate multi-dimensional seismic input motion vector for dynamic response analyses of spatial frame structures, it is necessary to make clear the multi-dimensional characteristics of the observed motions. Those characteristics have been discussed in relation to such as the principal axises, orbits and dominant directions of the motion vector at one point. Few investigations of those characteristics have been performed in connection with the relationship in the frequency domain between the 3-dimensional motion vectors observed at the different two points. The purpose of this work is to make clear the multi-dimensional seismic wave propagation in soil by examining correlations, transfer functions and coherence functions of motion vectors based on statistical analyses. Coherent waves are detected by examining correlations between the motion vectors by using the cross correlation analyses. For 3-dimensional motion vectors and their rotary spectra, transfer functions and coherence functions are estimated by using of the linear least square method in the frequency domain. The change of the directions of the motion vectors is also examined.

OUTLINE OF ARRAY SYSTEM AND OBSERVED EARTHQUAKES

The vertical instruments array was installed at Iwaki city which is located about 200km from Tokyo in Japan. Fig.1 shows the location of the observation points and the results of the PS-logging test(ref.1). Accelerometers were installed at every observation points. The outlines of the underground of the array site is shown in Fig.2. This figure indicates that the subsurface layers

dip slightly. The accelerograms used for the statistical analyses were observed by 18 earthquakes from November, 1981 to May, 1984. The magnitudes and epicenters of those earthquakes are shown in Fig.3.

CORRELATION BETWEEN MOTION VECTORS AT VERTICAL POINTS

In an attempt to detect types of waves which have high correlation between the orthogonal components(NS,EW,UD) of the motion vectors, we examine cross-correlation functions given as

$$C^{xy}{}_{i,j}(\tau)=\sum_{k=1}^{n}\left\langle \left(x_i^k(t)/\sqrt{I_k}\right)_{i,j=NS,EW,UD}\left(y_j^k(t+\tau)/\sqrt{I_k}\right)\right\rangle \quad \cdots(1)$$

$$I_k=\sum_{i=NS,EW,UD}\left\langle x_i^k(t)x_i^k(t)\right\rangle \quad \cdots(2)$$

where n is the sample number of earthquakes, the symbol(<>) represents time average, and $x_i(t)$ and $y_j(t)$ are i-component of motion vectors at x point and j-component at y point, respectively. Fig.4 shows the cross-correlation functions between the motion vector at the GL-330m point and the one at the GL-200m point in the matrix form. Those functions are normalized by the value of $C_{NS-NS}(0)$. The symbol(▽) indicates the peaks in those functions which we shall discuss. The time lags of the peaks of the different horizontal components are almost equal to 0.08 sec. and 0.12 sec. which are the theoretical traveling times of the vertical incident S-wave and its S-wave reflected at the surface, respectively. Those theoretical traveling times are calculated based on the S-wave velocity distribution(see Fig.1). This result can not be explained by the one dimensional wave propagation theory. The above results suggest the existence of multi-dimensional wave propagation. It is found that the values of the peaks in the cross-correlation function(see Fig.4-(d)) between the NS-component and the EW-component are negative. Those negative values will be discussed in later section.

TRANSFER FUNCTIONS AND COHERENCE FUNCTIONS FOR 3-DIMENSIONAL MOTION VECTORS

In order to derive the relationship in the frequency domain between any two components of the motion vectors at the different points, we estimate the transfer functions and coherence functions for the 3 dimensional motion vector by introducing the system with 3-inputs and 3-outputs. We suppose that every component of the motion vector at the output point is the sum of the contributions from each of the 3 components of the motion vector at the input point. The system(shown Fig.5) may be written as:

$$Y_i(w)=\sum_j H_{ij}(w)X_j(w)_{i,j=NS,EW,UD} \quad \cdots(3)$$

where H_{ij} is the element of transfer function matrix[H] and represents the contribution factor from the j input component to the i output component. By using the least square estimate method, [H] and coh(w) can be given in the form(ref.2).

$$[S^{xy}(w)]=[S^{xx}(w)]\,[H(w)]^t \quad \cdots(4) \qquad coh^2(w)=tr([H^*(w)]\,[S^{xy}(w)])/tr([S^{yy}(w)]) \quad \cdots(5)$$

where $[S_{xy}]$ and $[S_{xx}]$ are the cross spectral matrix between the motion vector at the input point and the one at the output point and the cross spectral matrix between components of the motion vector at the input point, respectively. We calculate the elements of $[S_{xy}]$ and $[S_{xx}]$ by taking the inverse Fourier transform of eq.(1). We estimate [H] and coh(w) of the system whose input point and output point are the GL-330m point and the GL-200m point,respectively. Fig.6 and Fig.7 show the amplitudes and the phase of the element of [H] estimated,respectively. The amplitude between the different components as well as those of the same components are dominant at about 1.2Hz which corresponds to the first natural frequency of the transfer function(Fig.8) calculated by the one dimensional wave

propagation model based on the S-wave velocity distribution(Fig.1). The shape of each amplitude is similar to the theoretical ones, except that the amplitudes of the different components convert to the values smaller than 1, as the frequency approach to zero. The phase of H_{EW-NS} is remarkably different from those of the others estimated and the theoretical transfer function. The initial phase of H_{EW-NS} is almost equal to 90 or -90 degree. On the other hand, those of the others are almost equal to zero degree. The above results can not be explained by the one dimensional wave propagation theory. This initial phase is necessary to be discussed in detail. Fig.9 shows that the values of the coherence function between the motion vectors are higher than between the same components. The above results suggest the existence of the multi-dimensional wave propagation.

TRANSFER FUNCTIONS FOR ROTARY COMPONENTS OF HORIZONTAL MOTION VECTORS

In order to discuss the negative values of the peaks of the cross correlation function and the initial phase of the transfer functions in the above results, we shall introduce the concept of the rotary spectra(ref.3) and examine the phase of the transfer function for the rotary spectrum of the horizontal motion vector. By representing the horizontal motion vector($X_{NS}(t)$,$X_{EW}(t)$) as the complex form

$$z(t)=x_{NS}(t)+ix_{EW}(t)=a(t)\exp(i\theta(t)) \qquad \cdots (6)$$

the rotary spectra (Fig.10) of the horizontal motion vector can be given in terms of the Fourier spectrum Z(w) of Z(t).

$$Z_+(w)=Z(w)=|Z_+(w)|\exp(i\theta_+(w))$$

$$Z_-(w)=Z(-w)=|Z_-(w)|\exp(i\theta_-(w)) \quad w>0 \qquad \cdots (7)$$

where $Z_+(w)$ and $Z_-(w)$ are the rotary spectrum component in the clockwise direction(see Fig.10) and that in the opposite direction, respectively. By using the least square method, we estimate the transfer function $H_r(w)$ and coherence function $coh_r(w)$ for Z_+ of the system with one input and one output illustrated in Fig.10. $H_r(w)$ and $coh_r(w)$ are given as

$$H_r(w)=S^{xy}{}_R(w)/S^{xx}{}_R(w) \qquad \cdots (8)$$

$$coh^2(w)=|S^{xy}{}_R(w)|^2/(S^{xx}{}_R(w)S^{yy}{}_R(w)) \qquad \cdots (9)$$

where the rotary cross spectrum S_r is calculated from the cross spectra($S^{ij}{}_{NS,NS}$, $S^{ij}{}_{NS,EW}$ and $S^{ij}{}_{EW,EW}$) of the orthogonal components by using the next equation.

$$S^{ij}{}_R(w)=S^{ij}{}_{NS.NS}(w)+S^{ij}{}_{EW.EW}+i(S^{ij}{}_{NS.EW}-S^{ij}{}_{EW.NS}) \quad i=x,y \quad j=x,y \qquad \cdots (10)$$

Fig.11 shows the amplitude and phase of the estimated transfer function. The amplitude of the rotary transfer function estimated is similar to that(Fig.8) of the one dimensional wave propagation model. However, the phase of H_r estimated and the theoretical one differ in the initial phase. Fig.12 indicates that this initial phase of H_r which varies in the soil is related to the change of the direction of the motion due to S waves. However, it is considered that directional errors of sensors such as in installment causes this initial phase. We shall discuss the effect of the directional errors to the initial phase. Supposing this initial phase as the directional errors of sensors and correcting the angle of the direction of the output motion vector by taking the transform of the output motion vector under rotation of coordinates system, let us examine the transfer functions for the corrected horizontal motion vector. Fig.13 shows the amplitudes and phase of the correlated transfer function matrix between the GL-330m point and GL-200m point. 35 degree which is the value of the correct angle is used. This value is calculated by taking the average of the initial phase angle(Fig.11-(b)) in the range from 0.2Hz to 0.6Hz. It is found that there is the remarkable transmission between the EW-component at the GL-200m point and the NS-component at the GL-330m point. This result indicates that the initial phase can not be explained only in terms of the directional errors of sensors. It is concluded that the initial phases are related to the multi-dimensional wave

propagation due to irregularities of the soil structure. For example, the dipping layer shown in Fig.2 is considered as the irregularities.

CONCLUSION

We discussed the multi-dimensional wave propagation by examining the transmission mechanism and correlation of the observed seismic motion vectors. It is shown that seismic waves propagate multi-dimensionally through subsurface layers with changing directions of motion vectors. This change can be explained in terms of irregularities of the soil structure. It is suggested that directions of multi-dimensional input motion vectors for earthquake response analyses of building structures are influenced by the soil structure as well as the direction of rupture propagation of seismic source.

ACKNOWLEDGMENT This array observation has been carried out by "Study on Characteristics of Seismic Motion in the Rock" founded by 6 electric power companies in Japan.

REFERENCES

1. Omote, S., Ohsawa, Y., Ohmura, B., Iizuka, S., Ohta, T. and Takahashi, K. "Observation of Earthquake Strong-Motion with Deep Boreholes - An Introductory Note for Iwaki and Tomioka Observation Station in Japan- ", 8WCEE, Vol.2, pp.247-254
2. Jenkns, G. M., Watts. D. G. "Spectral Analysis and it's applications", Holden-day, San Francisco,1968
3. Gonella, J. " A rotary-component method for analyzing meteorological and oceanographic vector time series", Deep-Sea Res., Vol.19, pp.289-269,1972

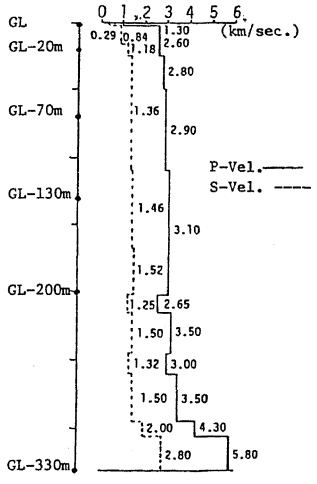

Fig.1 Obsevation points(O) and soil structure

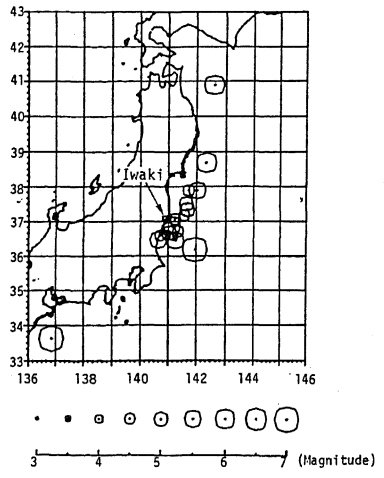

Fig.3 Epicenters and magnituedes of 18 earthquakes

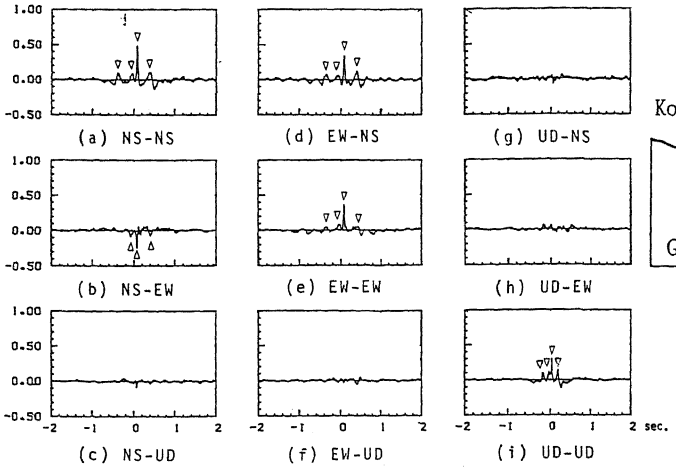

(horizontal axis: time lag(sec.))

Fig.4 Normalized cross correlation functions between GL-330m and GL-200m(:peak)

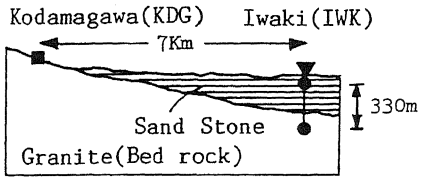

Fig.2 Outline of the undergound of the array

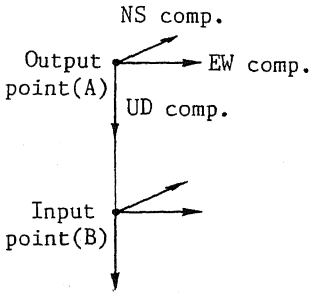

Fig.5 directions of motion vector at input point and output point

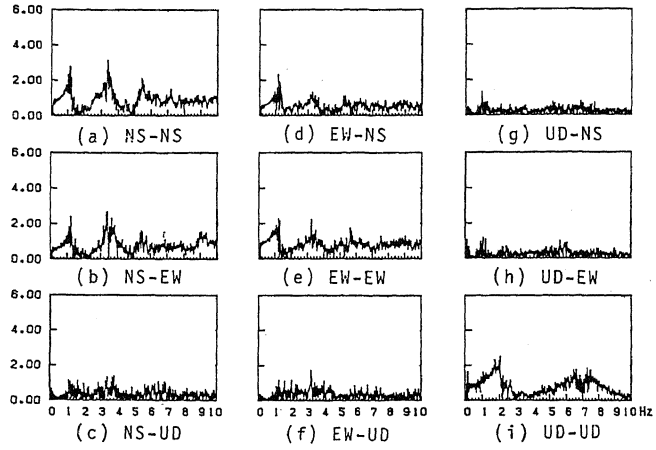

Fig.6 amplitudes of estimated transfer functions for 3 dimesional vector of motions based on system with 3-inputs and 3-outputs(input point: G1-330m output point:GL-200m)

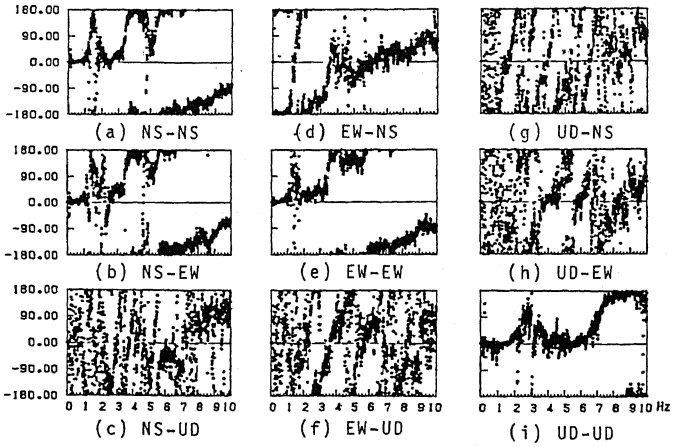

Fig.7 phases of transfer functions correspond to the amplitudes in Fig.6)

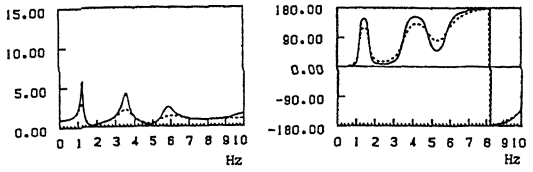

(a) amplitude (b) phase

Fig.8 transfer function of shear waves calculated based on one dimesional propagation

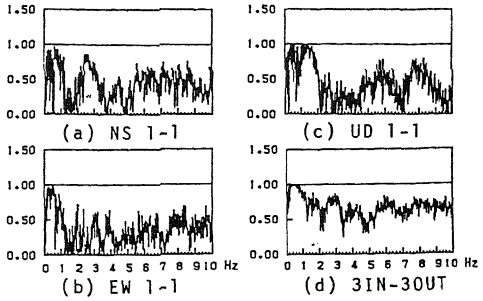

Fig.9 comparaion in coherence functions of motion with the same components(1-1) and 3 dimesional vectors(3-3)

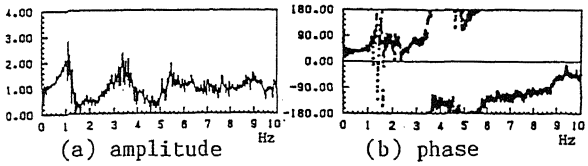

(a) amplitude (b) phase

Fig.11 transfer function for rotary spectral (input point:GL-330m output point:GL-200m)

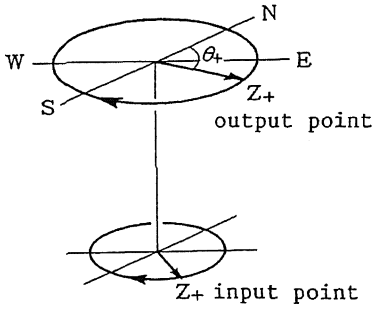

Fig.10 layout of the input-output system for the rotary spectrum.

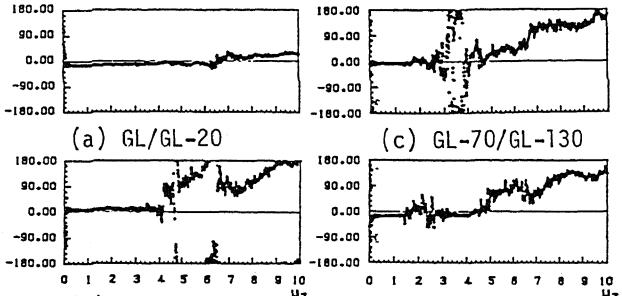

Fig.12 phase of the transfer functions for rotary spectrum(the symbol(A/B) indicates that A and B are output point and input point, respectively)

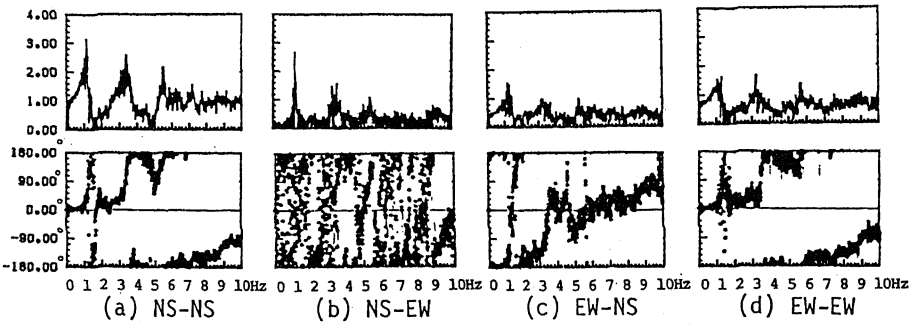

Fig.13 amplitudes and phases of estimated transfer functions for horizontal components corrected.